



Performance Analysis of Energy Efficient Spatial Modulation in Bidirectional Cooperative Cognitive Radio System with Eavesdropper

Renjith Ravindran Unnithan Jalaja¹ · P. G. S. Velmurugan¹ · S. J. Thiruvengadam¹

Accepted: 7 January 2022

© The Author(s), under exclusive licence to Springer Science+Business Media, LLC, part of Springer Nature 2022

Abstract

This paper examines the Secrecy Outage Probability (SOP) and outage performance of an energy efficient Spatial Modulation (SM) in a bidirectional Decode and Forward (DF) Cooperative Cognitive Radio (CCR) system with the presence of an eavesdropper. In the proposed system, both primary and secondary users use SM technique to enhance the spectral efficiency and energy efficiency of the bidirectional system. The two primary users swap their information with the aid of a secondary user, which acts as a bidirectional DF relay node. Time Switching Relaying protocol-based energy harvester is employed in the secondary user to harvest the energy from both SM operated primary users. Secondary user information is embedded with jamming signal to confuse the eavesdropper. The SOP of the primary user and secondary user are examined in the presence of an eavesdropper. Furthermore, the lower bound and upper bound outage probability of the proposed bidirectional CCR system with Physical Layer Network Coding and SM are derived with respect to the harvested energy. Simulation results are presented to provide the functional perception of the proposed system behavior and emphasize the effect of different system parameters.

Keywords Spatial modulation · Energy harvesting · Cognitive radio system · Secrecy outage probability

1 Introduction

In past two decades, wireless communication network has witnessed unprecedented development in information traffic, driven by the popularity of multiple smart devices, electronic gadgets, need for exuberant multimedia content, and the exponential increase in the number of Base Stations (BS). This resulted in a lack of range for fresh wireless devices and applications. 5G has evolved as a potential candidate in order to cope this spectrum deficiency and huge data traffic [1]. Spatial Modulation (SM), Energy Harvesting (EH), massive Multiple Input Multiple Output (MIMO), millimetre (mm) Wave, and Physical (PHY) Layer Security are some of the important technologies in 5G mobile communication networks

✉ Renjith Ravindran Unnithan Jalaja

¹ Present Address: Department of ECE, Thiagarajar College of Engineering, Madurai, India

[2]. SM increases the spectral efficiency and reduces the number of Radio Frequency (RF) chains, which activates only one antenna during the time slot [3]. SM carries two information units. One is the conventional modulation and other is the antenna index [4]. SM significantly elevates the system performance by using efficient detection methods [5]. SM is effectively used in MIMO systems to improve the energy efficiency [6]. The power allocation strategy for MIMO system and the total power constraint are investigated in [7]. In recent years, researchers focus on energy harvesting, which is one of the strong and potential parameter of the 5G wireless communication systems. Simultaneous Wireless Information and Power Transfer (SWIPT) deals that RF signal not only carries the information but also carry the energy [8] [9]. The EH process avoid the frequent charging of wireless gadgets and reduces the emission of carbon footprint [10]. There are two types of EH protocols, Time Switching Relaying (TSR) protocol and Power Splitting Relaying (PSR) protocol. In TSR scheme, the EH and information transmission depends on the fraction of time, while the PSR protocol performs the EH and information transmission concurrently [11].

The security paradigms that protect the confidentiality and authenticity of wireless transmission in the 5G network remains elusive despite current efforts by academic and industry researchers. Definitely, one of the key problems in any 5G network is how to secure the wireless data transmission. In [12] physical layer security for both PSR and TSR protocol is analyzed in unidirectional relay networks. Normally, all the data encryption standards and cryptographic algorithms are based on the perspective of application layer in the Open System Interconnection (OSI) model [13]. Differing from the conventional security approaches, Wyner laid the notion of PHY which provides the secure wireless transmissions by exploiting the characteristics of fundamental transmission medium without using any algorithms and keys [14]. Physical Layer Security (PLS) [15] is a very powerful tool to maintain the confidentiality without using key and achieving perfect secrecy rate. Cooperative communications plays a significant role in day to day life which increases the system capacity, network coverage and Quality of Service (QoS) through independent relaying path. This leverages the reliability of transmission by using diversity gain and spatial multiplexing [16]. An energy efficient fault tolerant scheme based on network coding is proposed to improve the wireless body area network [17].

Two way relaying is an efficient method to improve the capacity and energy efficiency of the system. Mainly there are two types of cooperative relaying methods such as Amplify and Forward (AF) and Decode and Forward (DF). In AF relay mechanism, the relay receives the information from the source and amplify the signal, forwards to the destination. Moreover, DF relay receives the signal from both the sources and decodes the symbol then broadcasts to the corresponding sources [18] [19]. In [20], the authors proposed the three step bidirectional information exchange of two source nodes with the leverage of energy harvested DF relay. The performance of co-operative relaying is a measure of throughput, outage probability and Quality of service (QoS) [21]. However, this cooperative communications have been integrated into most modern applications such as Physical layer security and Cognitive radio (CR) systems.

CR system is a promising solution to mitigate the effect of spectrum deficiency and underutilisation of spectrum [22]. CR system allows the spectrum sharing mechanism of Secondary User (SU) without degrading the performance of the Primary User (PU) link. Mainly, there are three types of spectrum sharing approach, they are overlay, underlay and interweave approaches [23]. Data rate and secrecy outage performance of a wireless relay system can be enhanced effectively with the aid of a novel method, Physical Layer Network Coding (PLNC) [24]. Interference in multi user MIMO system can be utilized to improve the SWIPT performance with the help of PLNC [25]. PLNC combines the symbol from

both the sources of a bidirectional relaying system. The SOP of a underlay cognitive radio network with EH in the presence of an eavesdropper and direct link is investigated in [26]. The EH relay based underlay CR system is proposed in [27] to minimise the SOP. The secrecy performance of an DF cognitive dual hop relaying with co channel interference is studied in [28]. The potential benefits of SM is applied to the cooperative communications to improve the spectral efficiency with minimum power consumption and receiver complexity. The implementation of SM in cooperative communications will enhance the spectral efficiency which is one of the potential requirements in next generation wireless communication networks [29].

To the best of authors knowledge no analysis have been carried out in the bidirectional aspect of spatial modulation based cooperative cognitive radio in the presence of an eavesdropper with energy harvesting. Future wireless scenarios are expected to be deployed in spectrum starved conditions also multi-fold increase in the shadowing probability between the nodes are expected. Hence, in this model primary users allows the secondary user to utilize their own spectrum (CR) and energy (EH), in return primary users expect the secondary user to act as intermediary relay to improve the reliability of the transmissions between primary user nodes. Hence, this paper proposes the performance investigations on outage probability and secrecy outage performance of bidirectional spatial modulated cooperative cognitive radio system with an eavesdropper.

The major contributions of this research paper is listed below,

- A novel energy efficient SM based bidirectional cooperative cognitive radio system with an eavesdropper is proposed. In this proposed system, primary users and secondary user (EH-relay) are spatial modulation enabled transceivers.
- For the proposed system, analytical expressions of the lower and upper bounds end to end outage probability are derived for the bidirectional link.
- Secrecy Outage Performance of the proposed system is numerically analyzed in the presence of a single eavesdropper.
- The effect of power splitting factor, power allocation factor is examined and contrasted with the performance of the proposed system without spatial modulation.

2 System Model

The SM based energy harvesting bidirectional cooperative cognitive radio system in the presence of an eavesdropper is shown in Fig. 1. In this proposed system, it is assumed that there is no direct link between the primary user nodes PU_1 and PU_2 due to the shadowing or large scale pathloss. The two primary user nodes PU_1 and PU_2 exchange their information in two time slots with the help of secondary user SU which acts as a half duplex DF relay node to combine the information from primary users using PLNC concept. The two primary user nodes PU_1 and PU_2 are equipped with N_t antennas and secondary user relay node SU is equipped with N_r antennas. Secondary receiver SU_{RX} and the eavesdropper are equipped with single antenna. SM is employed at both primary user nodes PU_1 , PU_2 and secondary user node which carries additional bit of information that increases the spectral efficiency of primary users and secondary user. In time slot I, primary user nodes PU_1 and PU_2 transmit $\log_2(N_t) + \log_2(M)$ bits to the secondary user, where M is the number of constellation point. The secondary user SU decodes and harvests the energy from spatial modulated information of two primary user nodes. The

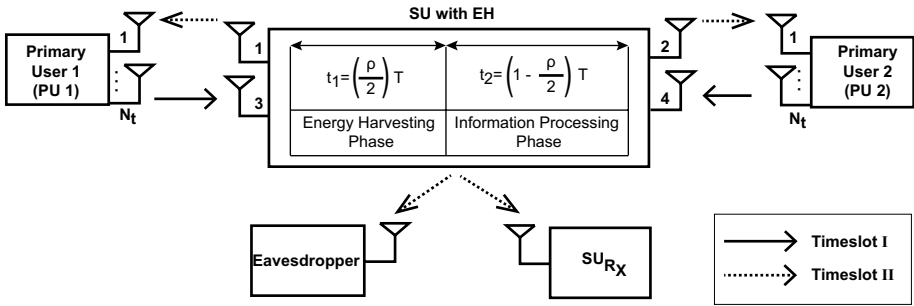


Fig. 1 System model for SM bidirectional Energy Harvested Cooperative Cognitive Radio system with eavesdropper

number of transmit antennas at secondary user node SU must satisfy $N_r = 2^{\log_2 N_t} + N_t$. In time slot II, the antenna selection at secondary user SU is based on the decimal equivalent of PLNC encoded primary user spatial modulated information. Secondary user node SU also transmits its own information and jamming signal to secondary receiver SU_{RX} . The jamming signal is to confuse the eavesdropper, which is in close proximity to secondary user SU . It is assumed that, both primary and secondary users have apriori information about the jamming signal. As legitimate nodes are familiar with the jamming signal, it can be suppressed. An example of PLNC encoding at both the time slots are provided in Table 1.

In time slot I, the $N_r \times 1$ received signal vector at secondary node SU is given by,

$$y_R = \sqrt{P_1} \mathbf{g}_{1R}^{q_1} x_1 + \sqrt{P_2} \mathbf{g}_{2R}^{q_2} x_2 + \mathbf{n}_R \tag{1}$$

where P_1 and P_2 denote the transmit powers at PU_1 , PU_2 respectively. $\mathbf{g}_{1R}^{q_1}$ and $\mathbf{g}_{2R}^{q_2}$ are the channel coefficients between primary user nodes PU_1 & SU and PU_2 & SU respectively, q_1 and q_2 are the transmitted antenna index which carry spatial information. The channel coefficients are modeled as independent and identically distributed Rayleigh random variables. For a block duration of time T , this channel is quasi static and reciprocal. x_1 and x_2 are the transmitted symbols from the primary user nodes PU_1 and PU_2 respectively. \mathbf{n}_R is Additive White Gaussian noise (AWGN), modeled as Zero mean circularly symmetric complex Gaussian (ZMCSCG) with variance σ_R^2 .

The secondary user SU equipped with Time Switching Relaying (TSR) protocol to carry out energy harvesting and information processing. The EH is carried out for $t_1 = \left(\frac{\rho}{2}\right)T$ sec duration and information processing for $t_2 = \left(1 - \frac{\rho}{2}\right)T$ sec duration, where ρ is the time proportion for energy harvesting and information processing and T is the total duration of time i.e. $(t_1 + t_2 = T)$ (see Fig. 1). The SU node decodes the spatial modulated primary user data, map the decimal equivalent value as antenna index

Table 1 Example of PLNC mapping

Time	Antenna information & M-ary	PLNC decoding
Slot- I	$PU_1 = 10, PU_2 = 11$	$q_R = 10 \oplus 11 = 01$
Slot- II	$q_R, x_S \rightarrow PU_i, SU_{RX}, i \in 1, 2$	$PU_1 = 01 \oplus 10 = 11$ $PU_2 = 01 \oplus 11 = 10$

and broadcasts its own data using the harvested energy. The energy harvested at the *SU* node during t_1 is given by,

$$E_h = \eta \lambda \left(P_1 \|\mathbf{g}_{1R}^{q_1}\|^2 + P_1 \|\mathbf{g}_{2R}^{q_2}\|^2 \right) \left(\frac{\rho}{2} \right) T \tag{2}$$

where η represents the energy efficiency factor of the circuit and λ is the power splitting factor. Applying time splitting policy in (2), the power of *SU* node is calculated as,

$$P_R = \frac{E_h}{\left(1 - \frac{\rho}{2}\right) T} = \frac{\eta \lambda \left[P_1 \|\mathbf{g}_{1R}^{q_1}\|^2 + P_1 \|\mathbf{g}_{2R}^{q_2}\|^2 \right] \frac{\rho}{2}}{\left(1 - \frac{\rho}{2}\right)} \tag{3}$$

The maximum likelihood detection criteria is applied at *SU* node to detect q_1, q_2, x_1 and x_2 . It is given by

$$(\hat{q}_1, \hat{q}_2, \hat{x}_1, \hat{x}_2) = \arg \min_{q_1, q_2, x_1, x_2} \left\| \mathbf{y}_R - \mathbf{g}_{1R}^{q_1} x_1 - \mathbf{g}_{2R}^{q_2} x_2 \right\|^2 \tag{4}$$

\hat{q}_1, \hat{q}_2 are the detected antenna indices and \hat{x}_1, \hat{x}_2 are the detected symbols of *PU*₁ and *PU*₂ respectively. The encoding of the antenna indices and the symbols at *SU* node is based on the PLNC principle, which is given by the pairwise ex-or operation of $q_R = \hat{q}_1 \oplus \hat{q}_2, \hat{x}_1 \oplus \hat{x}_2$.

During time slot II, the *SU* node forwards the decimal equivalent of q_R in spatial domain and its own x_S via M-ary constellation symbols. A jamming signal x_S^j is superimposed in the information phase of secondary user node in order to confuse the eavesdropper. Now, the $N_i \times 1$ received signal vector at the i^{th} primary nodes *PU*_{*i*} is given by,

$$\mathbf{y}_{PU_i} = \sqrt{\beta P_R} \mathbf{g}_{Ri}^{q_R} x_S + \sqrt{(1 - \beta) P_R} \mathbf{g}_{Ri}^{q_R} x_S^j + \mathbf{n}_{p_i}, i = 1, 2 \tag{5}$$

where β is the power allocation factor at the secondary user node, the factor $\sqrt{\beta P_R}$ allocate the power for transmitting the secondary user information and $\sqrt{(1 - \beta) P_R}$ for transmitting the jamming signal respectively. Here, the legitimate nodes, the primary user and secondary receiver have apriori knowledge about the jamming signal, so the legitimate nodes can easily subtract the jamming part and \mathbf{n}_{p_i} is the AWGN at the primary user nodes. Similarly, the received signals at the secondary receiver *SU*_{*RX*} and eavesdropper are expressed as,

$$y_S = \sqrt{\beta P_R} g_{RS}^{q_R} x_S + \sqrt{(1 - \beta) P_R} g_{RS}^{q_R} x_S^j + n_S \tag{6}$$

$$y_E = \sqrt{\beta P_R} g_{RE}^{q_R} x_S + \sqrt{(1 - \beta) P_R} g_{RE}^{q_R} x_S^j + n_E \tag{7}$$

where $g_{RS}^{q_R}, g_{RE}^{q_R}$ are the channel coefficients from the *SU* node to secondary user receiver, eavesdropper respectively and they are modelled as Rayleigh random variables. The jamming parts in (5) and (6) can be eliminated by the trusted users.

The maximum likelihood detection criteria at the primary user node *PU*_{*i*}, $i \in 1, 2$ to detect the spatial bit is expressed as,

$$\hat{q}_R = \arg \min_{q_R} \left\| \mathbf{y}_{PU_i} - \mathbf{g}_{Ri}^{q_R} \right\|^2, i = 1, 2 \tag{8}$$

\hat{q}_R is the detected symbols from the antenna indices, which embeds both the antenna index and information of primary user. The decoding of the spatial modulated symbol at primary user PU_1 is decoded as $\hat{q}_R \oplus \hat{q}_1 \hat{x}_1$ and PU_2 is decoded as $\hat{q}_R \oplus \hat{q}_2 \hat{x}_2$ respectively (see Table 1).

Furthermore, the detection criteria at the secondary receiver SU_{RX} to detect the M-ary bit is given by,

$$\hat{x}_S = \arg \min_{q_R \in \{1, 2, \dots, N_r\}} \left| y_S - g_{RS}^{q_R} x_S \right|^2 \quad (9)$$

3 Performance Analysis of the Proposed System

3.1 SOP Analysis

Secrecy Outage Probability (SOP) is defined as the probability that the secrecy capacity (C_S) falls below a predefined secrecy rate (R_S), which can be articulated as,

$$SOP = Pr[C_S < R_S] \quad (10)$$

the secrecy capacity is defined as the difference between the main channel capacity and eavesdropper channel capacity, follows as,

$$C_S = (C_m - C_e) \quad (11)$$

From (5), the average SNR at the primary user node PU_i , $i \in (1, 2)$ is expressed as,

$$\gamma_{PU_i} = \frac{\beta P_R \left\| \mathbf{g}_{Ri}^{q_R} \right\|^2}{\sigma_P^2}, i \in (1, 2) \quad (12)$$

where σ_P^2 is the noise variance of the primary user nodes. Similarly, from (7) the average SNR at the eavesdropper node (E) is written as follows,

$$\gamma_E = \frac{\beta P_R \left| g_{RE}^{q_R} \right|^2}{(1 - \beta) P_R \left| g_{RE}^{q_R} \right|^2 + \sigma_E^2} \quad (13)$$

Hence, the main channel capacity is expressed as [29],

$$C_m = \log_2 (1 + \gamma_{PU_i}) + \log_2 N_r, i \in (1, 2) \quad (14)$$

substituting γ_{PU_i} from (12), the capacity of the main channel is obtained as,

$$C_m = \log_2 \left(1 + \frac{\beta P_R \left\| \mathbf{g}_{Ri}^{q_R} \right\|^2}{\sigma_P^2} \right) + \log_2 N_r, i \in (1, 2) \quad (15)$$

Likewise, the eavesdropping channel capacity is given by,

$$C_e = \log_2(1 + \gamma_E) + \log_2 N_t \quad (16)$$

substituting γ_E from (13) obtain the capacity of the eavesdropper channel and it is expressed as,

$$C_e = \log_2 \left(1 + \frac{\beta P_R |g_{RE}^{q_R}|^2}{(1 - \beta) P_R |g_{RE}^{q_R}|^2 + \sigma_E^2} \right) + \log_2 N_t \quad (17)$$

Hence, from (10) the secrecy outage probability at the primary user nodes $PU_i, i \in (1, 2)$ is rewritten as,

$$\text{SOP}_{PU_i} = \Pr[(C_m - C_e) < R_S], i \in (1, 2) \quad (18)$$

substituting (15) and (17) in (18) secrecy outage probability at the primary user nodes $PU_i, i \in (1, 2)$ is given by,

$$\text{SOP}_{PU_i} = \Pr \left\{ \left(\log_2 \left(1 + \frac{\beta P_R \|g_{Ri}^{q_R}\|^2}{\sigma_P^2} \right) + (\log_2 N_t) \right) - \log_2 \left(1 + \frac{\beta P_R |g_{Ri}^{q_R}|^2}{(1 - \beta) P_R |g_{Ri}^{q_R}|^2 + \sigma_E^2} \right) + (\log_2 N_t) < R_S \right\}_{i \in (1, 2)} \quad (19)$$

Moreover, SOP at Secondary Receiver SU_{RX} is obtained as,

$$\text{SOP}_{SU_i} = \Pr \left\{ \left(\log_2 \left(1 + \frac{\beta P_R \|g_{RS}^{q_R}\|^2}{\sigma_S^2} \right) + (\log_2 N_t) \right) - \log_2 \left(1 + \frac{\beta P_R |g_{RE}^{q_R}|^2}{(1 - \beta) P_R |g_{RE}^{q_R}|^2 + \sigma_E^2} \right) + (\log_2 N_t) < R_S \right\} \quad (20)$$

However, to the authors knowledge both (19) and (20) cannot be evaluated as closed form solution. By the way, the numerical solutions are presented in Sect. 4.

3.2 Outage Probability Analysis

The end to end outage probability of the primary user nodes PU_1 and PU_2 are analyzed in this subsection.

3.2.1 Outage Probability at Secondary User Node

In the multiple access phase, the secondary user node receives the information from both the primary user nodes PU_1 and PU_2 , so the outage probability at the SU node is expressed as,

$$P_{out}^R = Pr(C < R_d) \tag{21}$$

where C is the channel capacity and R_d is the target data rate in bits/sec/Hz. In a bidirectional DF relay node, the outage probability is determined in terms of lower bound and upper bound outage probability [20]

Hence, the expression (21) is rewritten in terms of SNR as follows

$$P_{LB-out}^R = Pr[\log_2(1 + \max(\gamma_{1R}, \gamma_{2R})) + \log_2 N_t < R_d] \tag{22}$$

where γ_{1R}, γ_{2R} are the SNR at the SU node is given by $\gamma_{1R} = \frac{\|\mathbf{g}_{1R}^{q1}\|^2 P_1 (1-\lambda)}{\sigma_R^2}, \gamma_{2R} = \frac{\|\mathbf{g}_{2R}^{q2}\|^2 P_2 (1-\lambda)}{\sigma_R^2}$.

From (22) the lower bound outage probability at the SU node is simplified as,

$$P_{LB-out}^R = Pr[\max(\gamma_{1R}, \gamma_{BR}) < \gamma_1^{th}] \tag{23}$$

where $\gamma_1^{th} = 2^{R-\log_2 N_t} - 1$ is the predefined threshold. From (23) it can be seen that the channel coefficient in the SNR expression follows the Chi-squared distribution. Substituting the SNR values in (23) and the Chi-squared nature of the random variable, the above expression is further simplified and the lower bound outage probability at the SU node is written as,

$$P_{LB-out}^R = [1 - e^{-\alpha_1} (1 + \alpha_1)] [1 - e^{-\alpha_2} (1 + \alpha_2)] \tag{24}$$

where $\alpha_1 = \frac{\gamma_1^{th} \sigma_R^2}{(1-\lambda)P_1}$ and $\alpha_2 = \frac{\gamma_1^{th} \sigma_R^2}{(1-\lambda)P_2}$.

Likewise, the upper bound outage probability at the SU node is expressed as,

$$P_{UB-out}^R = Pr[\min(\gamma_{1R}, \gamma_{BR}) < \gamma_1^{th}] \tag{25}$$

substituting the SNR values in (25) and performing some mathematical operations the upper bound outage probability at the SU node is written as,

$$P_{UB-out}^R = 1 - [1 - (1 - e^{-\alpha_1} (1 + \alpha_1))] [1 - (1 - e^{-\alpha_2} (1 + \alpha_2))] \tag{26}$$

3.2.2 Outage Probability at Primary User Nodes

The outage probability at the primary user node $PU_i, i \in (1, 2)$ is evaluated as,

$$P_{out}^{PU_i} = Pr[\gamma_{PU_i} < \gamma^{th}] \tag{27}$$

From (12) the SNR at the primary user node PU_1 is rewritten as,

$$\gamma_{PU_1} = \frac{\beta P_R \|\mathbf{g}_{R1}^{qR}\|^2}{\sigma_P^2} \tag{28}$$

P_R is already expressed in (3). Substituting (3) in (28) the above expression (28) becomes

$$\gamma_{PU_1} = \frac{\beta\eta\lambda\rho \left[P_1 \|\mathbf{g}_{1R}^{q_1}\|^2 + P_2 \|\mathbf{g}_{2R}^{q_2}\|^2 \right] \|\mathbf{g}_{R1}^{q_R}\|^2}{2 \left(1 - \frac{\rho}{2} \right) \sigma_P^2} \tag{29}$$

The outage probability at the primary user node PU_1 is rewritten as,

$$P_{out}^{PU_1} = Pr[\gamma_{PU_1} < \gamma^{th}] \tag{30}$$

where $\gamma^{th} = 2^{R-\log_2 N_r} - 1$, let $b = \frac{(1-\frac{\rho}{2})2\sigma_P^2}{\beta\eta\lambda\rho}$ and substituting (29) in (30) and performing simple mathematical manipulations the outage probability at the primary user node PU_1 is obtained as,

$$P_{out}^{PU_1} = Pr \left[\|\mathbf{g}_{1R}^{q_1}\|^2 \leq \frac{b \gamma^{th}}{P_1 \|\mathbf{g}_{R1}^{q_R}\|^2} - P_2 \|\mathbf{g}_{2R}^{q_2}\|^2 \right] \tag{31}$$

Utilizing the probability condition, the expression (31) is further written as,

$$P_{out}^{PU_1} = \int_0^\infty Pr \left[\|\mathbf{g}_{1R}^{q_1}\|^2 \leq \frac{b \gamma^{th}}{P_1 x} - P_2 x \right] \times f_{\|\mathbf{g}_{R1}^{q_R}\|^2}(x) dx \tag{32}$$

The expression (32) is the combination of more than two random variables, hence to the best of authors knowledge the closed form solution of (32) does not exist. Hence, using the probability bound theory, it is written as in terms of lower bound outage probability ($P_{LB}^{PU_1}$) and upper bound outage probability ($P_{UB}^{PU_1}$) respectively [20],

$$P_{LB}^{PU_1} \leq Pr \left[P_1 \|\mathbf{g}_{1R}^{q_1}\|^2 + P_2 \|\mathbf{g}_{2R}^{q_2}\|^2 \leq \frac{b \gamma^{th}}{\|\mathbf{g}_{R1}^{q_R}\|^2} \right] \leq P_{UB}^{PU_1} \tag{33}$$

The lower bound outage probability at the primary user node PU_1 is expressed as,

$$P_{LB}^{PU_1} = Pr \left[2 \max(\|\mathbf{g}_{1R}^{q_1}\|^2, \|\mathbf{g}_{2R}^{q_2}\|^2) \leq \frac{b \gamma^{th}}{\|\mathbf{g}_{R1}^{q_R}\|^2} \right] \tag{34}$$

The expression (34) is further written as,

$$P_{LB}^{PU_1} = \int_0^\infty Pr \left(x \leq \frac{b \gamma^{th}}{2 \|\mathbf{g}_{R1}^{q_R}\|^2} \right) Pr \left(\|\mathbf{g}_{2R}^{q_2}\|^2 \leq \frac{b \gamma^{th}}{2 \|\mathbf{g}_{R1}^{q_R}\|^2} \right) \times f_{\|\mathbf{g}_{R1}^{q_R}\|^2}(x) dx \tag{35}$$

Evaluating the probability condition in (35) obtained as

$$P_{LB}^{PU_1} = \int_0^\infty \left(1 - e^{-\frac{b\gamma^{th}}{2x}} \left(1 + \frac{b\gamma^{th}}{2x} \right) \right) \left(1 - e^{-\sqrt{\frac{b\gamma^{th}}{2}}} \left(1 + \sqrt{\frac{b\gamma^{th}}{2}} \right) \right) \times xe^{-x} dx \tag{36}$$

Performing a few mathematical operations in (36) using [30], the lower bound outage probability at the primary user node PU_1 is expressed as,

$$P_{LB}^{PU_1} = \left[1 - e^{-\frac{b\gamma^{th}}{2}} \left(1 + \sqrt{\frac{b\gamma^{th}}{2}} \right) \right] \left[1 - \left(b\gamma^{th} K_2(\sqrt{2b\gamma^{th}}) + \frac{b\gamma^{th}}{2} \sqrt{2b\gamma^{th}} K_1(\sqrt{2b\gamma^{th}}) \right) \right] \tag{37}$$

Similarly, the upper bound outage probability at the primary user node PU_1 is depicted as,

$$P_{UB}^{PU_1} = Pr \left[2 \min \left(\|\mathbf{g}_{1R}^{q_1}\|^2, \|\mathbf{g}_{2R}^{q_2}\|^2 \right) \leq \frac{b\gamma^{th}}{\|\mathbf{g}_{R1}^{q_R}\|^2} \right] \tag{38}$$

According to the probability condition the equation (38) is further written as

$$P_{UB}^{PU_1} = \int_0^\infty Pr \left\{ 2 \min \left(x, \|\mathbf{g}_{2R}^{q_2}\|^2 \right) \leq \frac{b\gamma^{th}}{\|\mathbf{g}_{R1}^{q_R}\|^2} \right\} \times f_{\|\mathbf{g}_{R1}^{q_R}\|^2}(x) dx \tag{39}$$

Evaluating the probability condition in (39) obtained as

$$P_{UB}^{PU_1} = 1 - \int_0^\infty \left(e^{-\frac{b\gamma^{th}}{2x}} \left(1 + \frac{b\gamma^{th}}{2x} \right) \right) \left(e^{-\sqrt{\frac{b\gamma^{th}}{2}}} \left(1 + \sqrt{\frac{b\gamma^{th}}{2}} \right) \right) \times xe^{-x} dx \tag{40}$$

Integrating the expression (40) and performing mathematical simplifications the upper bound outage probability at the primary user node PU_1 is obtained as [30],

$$P_{UB}^{PU_1} = 1 - \left[\left(e^{-\sqrt{\frac{b\gamma^{th}}{2}}} \left(1 + \sqrt{\frac{b\gamma^{th}}{2}} \right) \right) \left(b\gamma^{th} K_2(\sqrt{2b\gamma^{th}}) + b\gamma^{th} \sqrt{\frac{b\gamma^{th}}{2}} K_1(\sqrt{2b\gamma^{th}}) \right) \right] \tag{41}$$

Hence, the end to end outage probability of the proposed system is given by,

$$P_{out-LB}^{end\ to\ end} = P_{LB-out}^R + \left[(1 - P_{LB-out}^R) P_{LB}^{PU_1} \right] \tag{42}$$

$$P_{out-UB}^{end\ to\ end} = P_{UB-out}^R + \left[(1 - P_{UB-out}^R) P_{UB}^{PU_1} \right] \tag{43}$$

4 Results and Discussions

In this section, the validation of the proposed system are done with the aid of analytical results, numerical and computer simulations. The simulation parameters of the proposed system are: Energy efficiency factor $\eta = 1$, power allocation factor $\beta = 0.5$, the distance between all the nodes are normalized to unity.

The impact of power allocation factor to the SOP at secondary receiver and primary receiver for different values of SNR is illustrated in Figs. 2 and 3 respectively. Initially, as the power allocation factor β increases the SOP starts to decrease. This is due to the fact that more power is allocated for main channel capacity and subsequently reduces the capacity of eavesdropper channel. From the plot, it is observed that the SOP reaches the minimum floor with gradual increase in β . After the minimum floor level, SOP slightly increases with the incremental value of β . In this scenario, more power is allocated for the processing of the information, obviously reduces the effect of jamming signal. Hence, dominant secrecy performance is achieved. The effect of SNR is also illustrated in these plots.

The variation of secrecy outage probability with power allocation factor of the proposed system is compared with an existing literature [26] in Fig. 4. The simulation parameter considered for the performance comparisons are: secrecy rate 0.3 bps/Hz and energy efficiency factor $\eta = 0.9$. It is observed that the existing literature provide SOP of 0.9 at power allocation factor $\beta = 0.2$, and in the proposed system model the SOP is 0.74 at the same

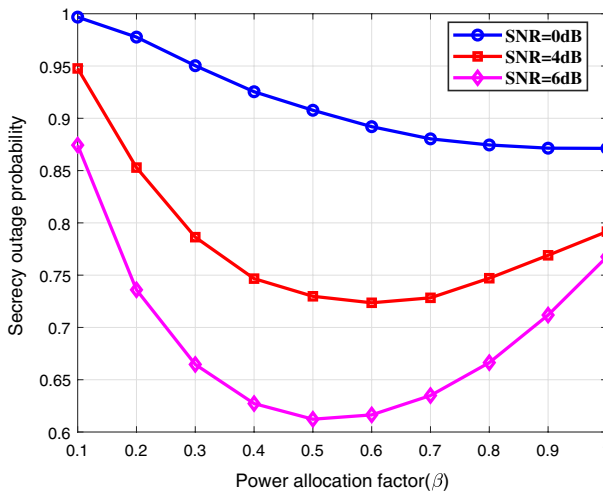


Fig. 2 SOP at secondary receiver versus power allocation factor β for different values SNR

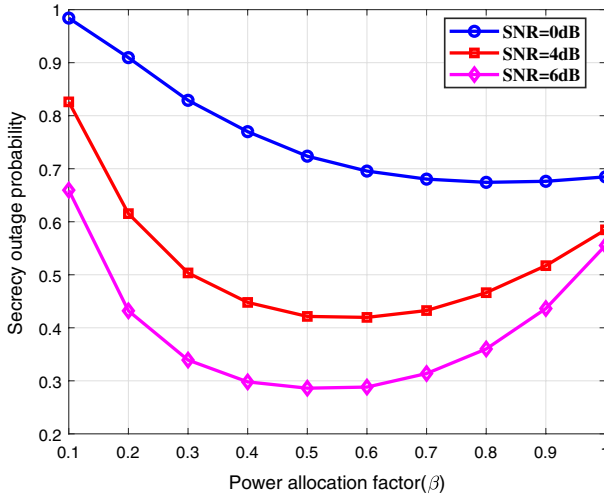


Fig. 3 SOP at primary receiver versus power allocation factor β for different values of SNR

power allocation factor. The parameter comparison between the proposed system and existing system model [26] is provided in Table 2.

The SOP at primary receiver with the power allocation factor for different antenna configurations $N_t = 2, 4, 6$ is illustrated in Fig. 5. From the plot, it can be seen that the number of antenna increases the system performs in an efficient way by the leverage of more number of independent path or diversity factor. Moreover, the optimal value of the power allocation factor can be easily chosen from the plot.

Power splitting factor λ of the energy harvester is varied and its impact on the end to end outage performance is depicted in Fig. 6. The analysis is also contrasted with the

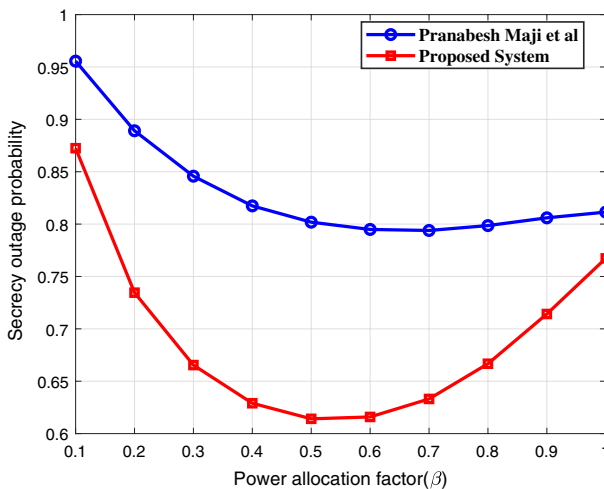


Fig. 4 Performance comparison of proposed system with an existing system model [26]

Table 2 Parameter comparison of proposed system with an existing system model [26]

Parameter for comparison	Proposed system	Existing literature [26]
Antenna configuration	SM-MIMO	SISO
Flow of information	Bidirectional	Unidirectional
CR approach	Spectrum sharing	Underlay
Analyzing criteria	SOP and outage probability	SOP only
Channel link	Relay link	Direct link and relay link
PLNC	Incorporated	Not incorporated

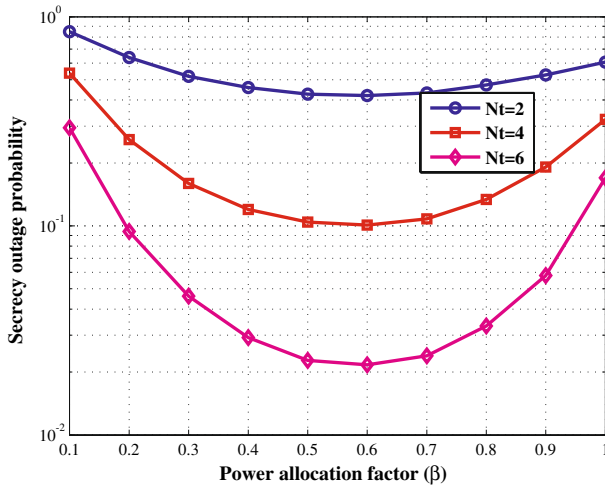


Fig. 5 SOP at primary receiver versus power allocation factor β for different antenna configurations N_t

system model without employing SM. The lower bound and upper bound outage probability of the proposed system is illustrated in this plot. Initially, the outage probability decreases with the gradual increase of λ to some optimal value (≈ 0.3). Further increasing the λ causes the outage probability to worsen. In fact, more power is used for energy harvesting in secondary user relay node and small amount of power is used for processing the information (see(42) and (43)).

The end to end outage probability of the proposed system with SNR is shown in Fig. 7. The proposed system is also compared with the system without assisting spatial modulation. From the plot, it can be seen that the SNR requirement to obtain 10^{-2} outage probability is 6 dB for SM lower bound, while in the case of without SM the same outage probability performance can achieved only at 11 dB. Since the outage probability

Fig. 6 End to end outage probability at primary user with power splitting factor λ

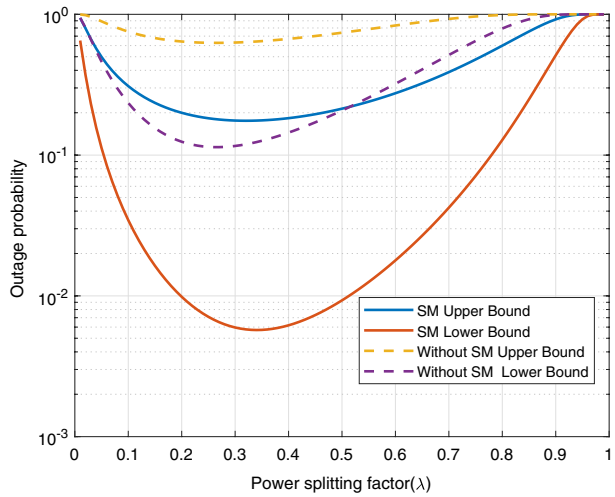
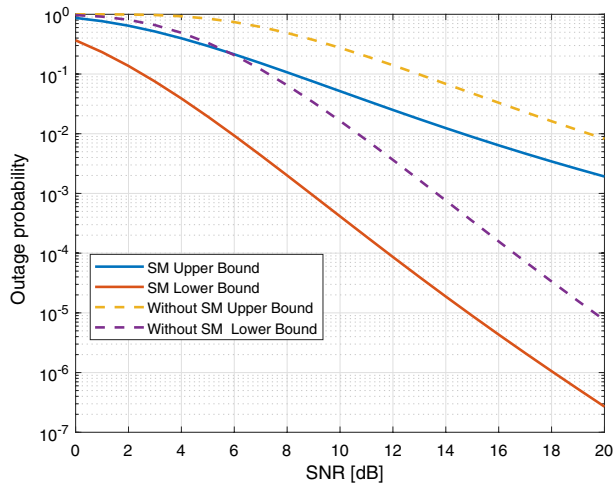


Fig. 7 Comparison of end to end outage probability at primary user with SM and without SM



is related to the channel capacity, therefore significant improvement is observed while employing SM in the proposed system

The energy harvesting capability of the proposed system under Rayleigh fading environment is given in Table 3. From the table it can be seen that, as the value of power splitting factor increases, more amount of energy is harvested (see(2)). Moreover, it may affect the information transmission capability of the system. Hence, the selection of λ value plays a vital role in energy harvesting and information processing of the proposed system.

Table 3 Energy harvesting trade-off of proposed system

Power splitting factor λ	Amount of energy harvested (J/s)
0.1	0.178
0.2	0.355
0.3	0.532
0.4	0.71
0.5	0.887
0.6	1.074
0.7	1.242
0.8	1.42
0.9	1.596
1	1.774

5 Conclusion and Future Work

In this paper, the outage probability of a bidirectional SM based energy harvested cooperative cognitive radio system with an eavesdropper is proposed. Two primary user nodes can communicate with the assistance of energy harvested relay using TSR protocol. The secrecy performance of both the primary user and secondary user is also investigated in this paper. The end to end outage probability of the proposed system is derived and plotted. The incorporated SM ensures better spectral efficiency, perfect secrecy, and the energy efficiency of the system is achieved by the process of energy harvesting at the relay node. Both spectral efficiency and energy efficiency are the key features of 5G wireless communication networks. The proposed system is more efficient in spectrum utilization with low energy requirement compared to the conventional cooperative systems. Furthermore, this scheme analyzed the physical layer security in terms of SOP in the presence of an eavesdropper. The incorporated power allocation factor plays a major role to improve the secrecy performance of the system. The impact of power allocation factor, power splitting factor on SOP and outage probability under Rayleigh fading environment is highlighted. This research proposal united the concept of cognitive radio, energy harvesting, spatial modulation, and physical layer security for the deployment of future cooperative wireless communications. Moreover, there exists a lot of open research problems such as the performance investigations on the proposed system with generalized fading channels and the analysis of cooperative cognitive radio system with full duplex relaying scheme. These open research problems can be addressed as the future work.

Data Availability The datasets analysed during the current study are not publicly available but are available from the corresponding author on reasonable request.

Declarations

Conflict of interest No funding was received to assist with the preparation of this manuscript. The authors declare that they have no conflict of interest.

References

1. Shiu, Y.-S., Chang, S., Wu, H.-C., Huang, S., & Chen, H.-H. (2011). Physical layer security in wireless networks: A tutorial. *IEEE Wireless Communications*, 18(2), 66–74.
2. Yang, N., Wang, L., Geraci, G., Elkashlan, M., Yuan, J., & Renzo, M. D. (2015). Safeguarding 5G wireless communication networks using physical layer security. *IEEE Communications Magazine*, 53(4), 20–27.
3. Mesleh, R., Haas, H., Sinanovic, S., Ahn, Chang Wook, & Yun, Sangboh. (2008). Spatial Modulation. *IEEE Transactions on Vehicular Technology*, 57(4), 2228–2241.
4. Basar, E. (2016). Index modulation techniques for 5G wireless networks. *IEEE Communications Magazine*, 54(7), 168–175.
5. Jeganathan, J., Ghrayeb, A., & Szczecinski, L. (2008). Spatial modulation: Optimal detection and performance analysis. *IEEE Communications Letters*, 12(8), 545–547.
6. Zhang, M., Miao, W., Shen, Y., Huang, J., Zhang, S., Zeng, Z., et al. (2019). Joint spatial modulation and beamforming based on statistical channel state information for hybrid massive mimo communication systems. *IET Communications*, 13(10), 1458–1464.
7. Yang, P., Xiao, Y., Xiao, M., Zhu, J., Li, S., & Xiang, W. (2019). Enhanced receive spatial modulation based on power allocation. *IEEE Journal of Selected Topics in Signal Processing*, 13(6), 1312–1325.
8. Liu, Y. (2016). Wireless information and power transfer for multirelay-assisted cooperative communication. *IEEE Communications Letters*, 20(4), 784–787.
9. Khandaker, M. R., & Wong, K.-K. (2014). Swipt in miso multicasting systems. *IEEE Wireless Communications Letters*, 3(3), 277–280.
10. Zeng, Y., & Zhang, R. (2015). Full-duplex wireless-powered relay with self-energy recycling. *IEEE Wireless Communications Letters*, 4(2), 201–204.
11. Nasir, A. A., Zhou, X., Durrani, S., & Kennedy, R. A. (2013). Relaying protocols for wireless energy harvesting and information processing. *IEEE Transactions on Wireless Communications*, 12(7), 3622–3636.
12. Lee, K., Bang, J., & Choi, H.-H. (2020). Secrecy outage minimization for wireless-powered relay networks with destination-assisted cooperative jamming. *IEEE Internet of Things Journal*, 8(3), 1467–1476.
13. Diffie, W., & Hellman, M. (1976). New directions in cryptography. *IEEE Transactions on Information Theory*, 22(6), 644–654.
14. Wyner, A. D. (1975). The wire-tap channel. *Bell System Technical Journal*, 54(8), 1355–1387.
15. Hamamreh, J. M., Furqan, H. M., & Arslan, H. (2018). Classifications and applications of physical layer security techniques for confidentiality: A comprehensive survey. *IEEE Communications Surveys and Tutorials*, 21(2), 1773–1828.
16. Laneman, J., Tse, D., & Wornell, G. (2004). Cooperative diversity in wireless networks: Efficient protocols and outage behavior. *IEEE Transactions on Information Theory*, 50(12), 3062–3080.
17. Mehmood, G., Khan, M. Z., Abbas, S., Faisal, M., & Rahman, H. U. (2020). An energy-efficient and cooperative fault-tolerant communication approach for wireless body area network. *IEEE Access*, 8, 69134–69147.
18. Mao, M., Cao, N., Chen, Y., & Zhou, Y. (2015). Multi-hop relaying using energy harvesting. *IEEE Wireless Communications Letters*, 4(5), 565–568.
19. Rabie, K. M., Adebisi, B., & Alouini, M.-S. (2017). Half-duplex and full-duplex af and df relaying with energy-harvesting in log-normal fading. *IEEE Transactions on Green Communications and Networking*, 1(4), 468–480.
20. Van, N. T. P., Hasan, S. F., Gui, X., Mukhopadhyay, S., & Tran, H. (2016). Three-step two-way decode and forward relay with energy harvesting. *IEEE Communications Letters*, 21(4), 857–860.
21. Shrestha, S., & Chang, K. (2008). Analysis of outage capacity performance for cooperative df and af relaying in dissimilar rayleigh fading channels. In: *2008 IEEE International Symposium on Information Theory*, vol. 1. IEEE, 494–498.
22. Xu, D., Yu, X., Sun, Y., Ng, D. W. K., & Schober, R. (2020). Resource allocation for irs-assisted full-duplex cognitive radio systems. *IEEE Transactions on Communications*, 68(12), 7376–7394.
23. Aswathi, V., & Babu, A. (2021). Performance analysis of noma-based underlay cognitive radio networks with partial relay selection. *IEEE Transactions on Vehicular Technology*, 70(5), 4615–4630.
24. Lu, K., Fu, S., Qian, Y., & Chen, H.-H. (2009). On capacity of random wireless networks with physical-layer network coding. *IEEE Journal on Selected Areas in Communications*, 27(5), 763–772.
25. Chan, T.-T., & Lok, T.-M. (2021). Utilizing interference by network coding for simultaneous wireless information and power transfer. *IEEE Wireless Communications Letters*, 10(6), 1349–1353.

26. Maji, P., Roy, S. D., & Kundu, S. (2018). Physical layer security in cognitive radio network with energy harvesting relay and jamming in the presence of direct link. *IET Communications*, 12(11), 1389–1395.
27. Banerjee, A., Maity, S. P., & Roy, S. (2018). On outage secrecy minimisation in an energy harvesting relay assisted cognitive radio networks. *IET Communications*, 12(18), 2253–2265.
28. Yang, Q., Ding, J., & Hu, A. (2019). Secrecy outage performance analysis of df cognitive relay network with co-channel interference. *Wireless Personal Communications*, 107(1), 549–564.
29. Li, Q., Wen, M., Basar, E., Poor, H. V., & Chen, F. (2019). Spatial modulation-aided cooperative noma: Performance analysis and comparative study. *IEEE Journal of Selected Topics in Signal Processing*, 13(3), 715–728.
30. Gradshteyn, I. S., & Ryzhik, I. M. (2014). *Table of integrals, series, and products*. Cambridge: Academic press.

Publisher's Note Springer Nature remains neutral with regard to jurisdictional claims in published maps and institutional affiliations.



Renjith Ravindran Unnithan Jalaja is a doctoral candidate at the signal processing lab Thiagarajar College of Engineering, Madurai. under AICTE-QIP scheme. He completed his masters in Jayaram College of Engineering and Technology, Trichy. His primary research focus is investigating Energy Harvesting and SWIPT systems and has keen interest in Index Modulation



P. G. S. Velmurugan is an Assistant Professor at the department of Electronics and Communication at Thiagarajar College of Engineering, Madurai. He completed his Ph.D. in Information and Communication (2015) under Anna University. His research interests include Physical Layer Network Coding, Bidirectional Co-operative Communications and Convex Optimization.



S. J. Thiruvengadam received the B.E. degree in Electronics and Communication Engineering from the Thiagarajar College of Engineering, Madurai, India, in 1991, the M.E. degree in Applied Electronics from College of Engineering-Guindy, Chennai, India, in 1994, and the Ph.D. degree from Madurai Kamaraj University, Madurai, in 2005. From January to December 2008, he was a Visiting Associate Professor with the Department of Electrical Engineering, Stanford University, Stanford, CA, under a Postdoctoral Fellowship, by the Department of Science and Technology, Government of India. He is currently Professor & Dean (Academics) with the Department of Electronics and Communication Engineering, Thiagarajar College of Engineering. His areas of research interest include Statistical Signal Processing and MIMO Wireless Communications.